



Bin-Carver: Automatic recovery of binary executable files

Scott Hand^a, Zhiqiang Lin^{a,*}, Guofei Gu^b, Bhavani Thuraisingham^a

^a Department of Computer Science, The University of Texas at Dallas, USA

^b Department of Computer Science and Engineering, Texas A&M University, USA

A B S T R A C T

Keywords:

File carving
ELF
Fragmentation
Digital forensics
File recovery
Binary code analysis

File carving is the process of reassembling files from disk fragments based on the file content in the absence of file system metadata. By leveraging both file header and footer pairs, traditional file carving mainly focuses on document and image files such as PDF and JPEG. With the vast amount of malware code appearing in the wild daily, recovery of binary executable files becomes an important problem, especially for the case in which malware deletes itself after compromising a computer. However, unlike image files that usually have both a header and footer pair, executable files only have header information, which makes the carving much harder. In this paper, we present Bin-Carver, a first-of-its-kind system to automatically recover executable files with deleted or corrupted metadata. The key idea is to explore the *road map information* defined in executable file headers and the *explicit control flow paths* present in the binary code. Our experiment with thousands of binary code files has shown our Bin-Carver to be incredibly accurate, with an identification rate of 96.3% and recovery rate of 93.1% on average when handling file systems ranging from pristine to chaotic and highly fragmented.

© 2012 Z. Lin, S. Hand, G. Gu & B. Thuraisingham. Published by Elsevier Ltd. All rights reserved.

1. Introduction

File carving (Pal et al., 2003, 2008; Garfinkel, 2007) is a process by which raw data is examined with the goal of reconstructing previously indexed files when file system metadata such as super-blocks, directory entries (`dentry`), and index-node (`inode`) tables are corrupted or missing. File carving is feasible because, when most operating systems delete a file, the file's content is not overwritten; only the metadata is affected. This is partly due to the fact that file systems are optimized for performance and protecting their security and privacy is not a primary concern.

File carving has largely been used for data recovery (Pal and Memon, 2009) (a lucrative market recently), such as restoring deleted files or recovering data from a damaged device. The need for this utility stems from the fact that end-users sometimes unintentionally “permanently”

delete a file, and sometimes disk directory content is corrupted (by malware for instance). File carving is also useful for digital forensics (Garfinkel, 2007), as it can recover evidence files that have been “deleted” by criminals.

File carving, theoretically a permutation problem, is challenging for several reasons. For example, it is often difficult to determine where files begin and end without some sort of data block index to provide the block order for a single file. Moreover, even though we can detect the start and end of a file, it is still not sufficient because of fragmentation (Garfinkel, 2007), which can cause a contiguous sequence of file blocks to be split into two or more contiguous sequences.

Traditional file carving techniques utilize header-footer pairs to identify file boundaries, leading to the recovery of files that are contiguous on the media (Pal et al., 2003, 2008; Garfinkel, 2007; Pal and Memon, 2009). For example, all JPEG files begin with the hexadecimal sequence `FF D8` and end with `FF D9` (Jpeg file interchange format file format summary). By looking for this kind of unique sequences, this approach is effective for certain types of files

* Corresponding author.

E-mail address: zhiqiang.lin@utdallas.edu (Z. Lin).

containing reliable header-footer signatures (such as JPEG files) in the absence of fragmentation. However, it is weak when applied to heavily fragmented files or those without exact header and footer information.

Meanwhile, traditional file carving focuses mainly on files of common forensic interest such as documents (e.g., TXT/DOC/PDF), images (e.g., JPEG/GIF/PNG), audio (e.g., WAV/WMF/MP3), and video (e.g., AVI/MPEG/MP4) files (Garfinkel, 2007; Pal and Memon, 2009). Fewer attempts have been made toward the recovery of binary executables. However, binary executable recovery is also useful. At the very least it can narrow down the search of the traditional carving space. That is, when given a disk image, we can exclude the binary executable files if we can identify them and only focus on other chunks of the disk.

On the other hand, binary executable carving has become an important concern recently to security and forensic investigation. This is because in the past few years, we have witnessed an exponential increase of malicious executable files. For example, according to a report from AV-Test (Year-end malware stats from av-test), they processed an average of 54k malware samples daily in 2010 (up from an average of 33k in 2009, and 426 in 1998). Furthermore, malware code often deletes itself (to remove its footprints) after accomplishing certain tasks. It is therefore helpful to have an approach with which executable files on a disk image can be enumerated, mapped, and recovered.

Thus, in this paper, as a first-in-its-kind proof-of-concept for binary executable file carving, we present a novel system, Bin-Carver, to focus in particular on ELF executables in the Linux/UNIX platform (Note that PE (Microsoft pe and coff specification) files for Windows share the same methodology as ELF files for UNIX and thus can be handled in a similar way). Our system is fully automatic. The key idea is not only that it explores the file structure information from the ELF headers, but also that it explores the intrinsic characteristics of the binary code such as the code distributions and the explicit control flow path present in the code. In particular, inspired by the image file carving which uses magic numbers to identify both headers and footers, we use magic numbers to first identify ELF headers, which will serve as a road map to recover all other sections/segments (Executable and linkable format). Because of fragmentation, the ELF header alone is not sufficient, and we further explore the binary code content. We especially focus on the explicit function call control flow path as a guideline with which to efficiently solve the fragmentation problem.

Bin-Carver focuses on the recovery of the binary code for the widely used x86 architecture. Since we leverage the internal control flow path of the binary code to handle fragmentation, it would appear that we have to solve the disassembly problem, which is challenging because x86 instructions could start at any address (i.e., there is no address alignment constraint). Fortunately, by looking at the code distributions, we find that the code sequence of the function call control flow path has unique signatures. Thus, Bin-Carver will not disassemble all of the binary code; it will only inspect a small amount to construct the control flow.

The main contribution of this paper is summarized as follows:

- We make the first step in recovering fragmented executable files in a disk image.
- We present the use of the *road map information* defined in executable file headers and the *explicit control flow paths* contained in the binary code to guide the recovery of the executable file.
- We have implemented a tool called Bin-Carver, and applied it to recover thousands of binary executables from a number of disk images. Our experimental results show that our technique achieves extraordinary accuracy even with large fragmentation.

2. Approach overview

In this section, we first define our file carving problem, then outline the challenges, and finally provide an overview of our system.

2.1. Problem statement and assumptions

In this paper, we aim to recover an ELF executable file e from a disk image D in the presence of only the file content blocks. Meanwhile, we only focus on recovery of the file content and do not attempt to recover its filename. For proof-of-concept and simplicity, we assume a Linux platform with EXT2 file system and block size 4K. It is important to note that, while newer file systems such as EXT3 and EXT4 are more commonly used in Linux machines recently, there is no difference in how the data blocks are laid out. EXT3 and EXT4 add improvements such as journaling and higher-level metadata that helps reduce fragmentation, but core structures remain similar enough that file carving accuracy is the same. EXT2 is used because its relative simplicity is useful in writing tools to evaluate accuracy.

We also assume the file content has not been overwritten. In addition, we assume the file content is stored in an increasing order in the disk. While this may not always be the case, we believe that violations of this assumption are rare enough that we can ignore the possibility for the purpose of evaluating this algorithm. At least in our evaluation with the EXT2 file system, we did not encounter such a case.

More formally, as illustrated in Fig. 1, assume that for an ELF file e that has n blocks in the disk, our goal is to *link* these n blocks together to eventually recover the files. As

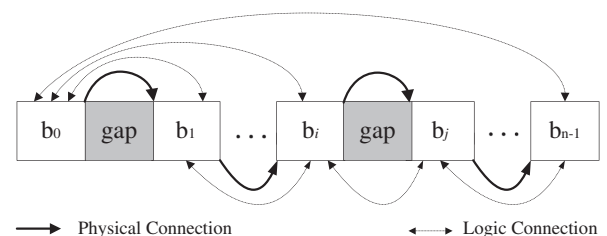


Fig. 1. Illustration of our file carving problem.

such, our solution is a graph-based approach. In particular, we utilize the internal logic between graph nodes to connect the data blocks. Note that the block address $A(b_j)$ is greater than $A(b_i)$ (the increasing order assumption), and there may be zero, one, or more data “garbage” gaps with size 4K each between the data block b_i and b_j where $i, j \in \{0, n - 1\}$.

2.2. Challenges

In the absence of file system metadata such as the `inode` and `dentry`, file carving is challenging. For instance, we cannot recover the filename that is managed in the `dentry` even though the `dentry` is not corrupted (overwritten). We made a detailed case study in the EXT2 file system (our experimental file system) and found that the `inode` pointer is cleared in the corresponding `dentry`. Consequentially, we cannot correlate any `dentry` with the `inode` to recover the filename. That explains why most file carving systems cannot recover filenames.

However, the most challenging problem is the fragmentation. A study by Garfinkel in 2007 (Garfinkel, 2007) showed that 15% of binary executables were found to be fragmented. However, in our experiments with EXT2 file systems, we discovered that the incidence of non-contiguous data block sequences is commonly even higher. For example, we took a `/bin/ls` binary with 92,376 bytes (requiring at least 23 4K data blocks) and observed how this binary file gets organized in a brand new disk. We found that this simple `ls` file actually gets fragmented (not stored contiguously) in the disk. In particular, we found this file requires 24 data blocks and there is a special data block which stores the pointer to the other data blocks. An investigation with the EXT2 file system data structure reveals that the 13th data block stores the one-layer indirect data block pointers. Therefore, in an EXT2 file system with 4K data blocks, the probability for a file with size larger than 48K being fragmented is very high, because there are only 12 direct data block pointers in the `inode`.

An intuitive approach that filters the indirect block by looking at the block content may be able to solve this problem. However, there are many other situations that can cause disk fragmentation. For example, on a disk already exhibiting a large degree of fragmentation, storing large files or appending data to existing files may further increase fragmentation, because there may not be a sufficient number of contiguous data blocks to store the new data.

2.3. System overview

An overview of our system is presented in Fig. 2. There are three key components in our system: *ELF-header scanner*, *block-node linker*, and *conflict-node resolver*. As the first step, *ELF-header scanner* is used to scan all possible ELF headers h_i using the ELF-file magic value. After that, guided by the road map from each h_i and the internal control flow of the binary code, *block-node linker* scans the disk image and tries to identify all the possible nodes and link them together. Finally, our *conflict-node resolver* will remove the conflict nodes introduced by our linker due to the

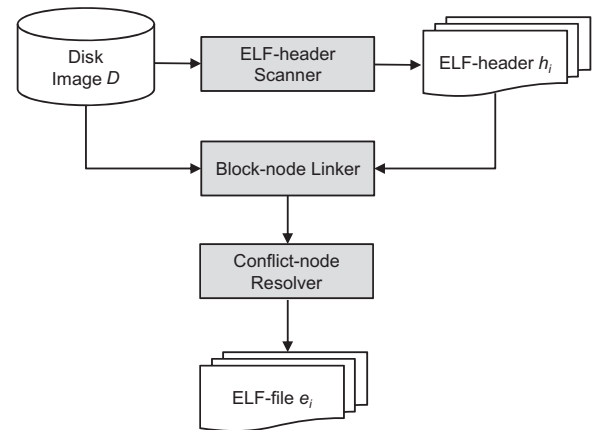


Fig. 2. System overview of our Bin-Carver.

fragmentation or possible garbage data to eventually output the ELF-file e_i .

3. Bin-Carver design

3.1. ELF-header scanner

The ELF header always resides at the beginning of an ELF file data block, and holds a “road map” describing the organization of an ELF file (Executable and linkable format). By searching for the magic number sequence `7f 45 4c 46` (.ELF) at the starting address of each data block (4K in our case) in D , we are able to locate the ELF headers, which contain a wealth of information on how to traverse all other code/data sections.

```

typedef struct {
00 unsigned char e_ident [16];
16 Elf32_Half e_type;
18 Elf32_Half e_machine;
20 Elf32_Word e_version;
24 Elf32_Addr e_entry;
28 Elf32_Off e_phoff;
32 Elf32_Off e_shoff;
36 Elf32_Word e_flags;
40 Elf32_Half e_ehsize;
42 Elf32_Half e_phentsize;
44 Elf32_Half e_phnum;
46 Elf32_Half e_shentsize;
48 Elf32_Half e_shnum;
50 Elf32_Half e_shstrndx;
} Elf32_Ehdr;
  
```

In particular, according to the above ELF header definition, each ELF header has 52 bytes, and it specifies the file offset of the *program header table* (PHT) and *section header table* (SHT). As shown in Fig. 3, for our working example `ls` binary, the PHT (an array of program headers) starts at address `0x34 00 00 00` (52 bytes into file) and SHT (an array of section header) starts at address `78 64 01 00` (91,256 bytes into file). It also tells us that this binary code

00000000	7f 45 4c 46 01 01 01 00	00 00 00 00 00 00 00 00	
00000010	02 00 03 00 01 00 00 00	80 9a 04 08 34 00 00 00	ELF Header
00000020	78 64 01 00 00 00 00 00	34 00 20 00 08 00 28 00	
00000030	1c 00 1b 00 06 00 00 00	34 00 00 00 34 80 04 08	Program Header
00000040	34 80 04 08 00 01 00 00	00 01 00 00 05 00 00 00	
00000050	04 00 00 00 03 00 00 00	34 01 00 00 34 81 04 08	
00000060	34 81 04 08 13 00 00 00	13 00 00 00 04 00 00 00	
00000130	04 00 00 00 2f 6c 69 62	2f 6c 64 2d 6c 69 6e 75	sec[1].interp
00000140	78 2e 73 6f 2e 32 00 00	04 00 00 00 10 00 00 00	sec[2].note.ABI-tag
00000150	01 00 00 00 47 4e 55 00	00 00 00 00 02 00 00 00	
00000160	06 00 00 00 08 00 00 00	61 00 00 00 68 00 00 00	...
000014b0	ff 35 08 e1 05 08 ff 25	0c e1 05 08 00 00 00 00	
000014c0	ff 25 10 e1 05 08 68 00	00 00 00 e9 e0 ff ff ff	sec[12].plt
00001a70	ff 25 7c e2 05 08 68 d8	02 00 00 e9 30 fa ff ff	
00001a80	31 ed 5e 89 e1 83 e4 f0	50 54 52 68 60 9e 05 08	sec[13].text
00016390	6c 73 00 00 52 a8 bd 5a	00 2e 73 68 73 74 72 74	
000163a0	61 62 00 2e 69 6e 74 65	72 70 00 2e 6e 6f 74 65	sec[27].shstrtab
00016470	75 67 6c 69 6e 6b 00 00	00 00 00 00 00 00 00 00	
00016480	00 00 00 00 00 00 00 00	00 00 00 00 00 00 00 00	
000164a0	0b 00 00 00 01 00 00 00	02 00 00 00 34 81 04 08	Section Header
000164b0	34 01 00 00 13 00 00 00	00 00 00 00 00 00 00 00	
000168c0	98 63 01 00 df 00 00 00	00 00 00 00 00 00 00 00	
000168d0	01 00 00 00 00 00 00 00		

[Nr]	Name	Type	Addr	Off	Size	ES	Flg	Lk	Inf	Al
[0]		NULL	00000000	000000	000000	00	0	0	0	0
[1]	.interp	PROGBITS	08048134	000134	000013	00	A	0	0	1
[2]	.note.ABI-tag	NOTE	08048148	000148	000020	00	A	0	0	4
[12]	.plt	PROGBITS	080494b0	0014b0	0005d0	04	AX	0	0	4
[13]	.text	PROGBITS	08049a80	001a80	0104bc	00	AX	0	0	16
[14]	.fini	PROGBITS	08059f3c	011f3c	00001c	00	AX	0	0	4
[15]	.rodata	PROGBITS	08059f60	011f60	003e4c	00	A	0	0	32
[27]	.shstrtab	STRTAB	00000000	016398	0000df	00	0	0	1	

Fig. 3. Data layout of our ls binary.

has 8 program headers with 32 bytes each, 28 section headers with 40 bytes each, and the section header string table index is at 27.

Searching SHT As can be seen in Fig. 3, the SHT is usually at the end of an ELF file (our profile with over 1K binaries in /bin and /usr/bin directory also confirmed this). Thus, as each ELF binary file has a well-defined ELF header, and from the header we can locate the logical address of the SHT (which could serve as a footer), that is $L(\text{footer})$ equals 78 64 01 00 (91256) in our working example. As a result, we need to search the disk to identify the footer.

Meanwhile, since $L(\text{footer})$ equals 78 64 01 00, then we only need to search the disk starting at the 0x14-th disk block (as our data block size is 4K) from the block of our ELF-header h_i because $A(\text{footer}) > A(h_i)$. In addition, we have another constraint from the ELF header that our footer is starting at the offset 0x678 of the potential data block, and that it has 28 entries (indicated in the ELF header) with 40 bytes each ($\text{sizeof}(\text{Elf32_Shdr})=40$).

Now we must derive a value invariant signature (Dolan-Gavitt et al., 2009) for the section header. Fortunately, section headers do have a unique signature. Specifically, using the section header data structure definition below,

```
typedef struct {
00 Elf32_Word sh_name;
04 Elf32_Word sh_type;
08 Elf32_Word sh_flags;
12 Elf32_Addr sh_addr;
16 Elf32_Off sh_offset;
20 Elf32_Word sh_size;
24 Elf32_Word sh_link;
28 Elf32_Word sh_info;
```

```
32 Elf32_Word sh_addralign;
36 Elf32_Word sh_entsize;
} Elf32_Shdr;
```

from the documentation of ELF structure (Executable and linkable format), we check the following:

- $V(\text{sh_name}) \in \{0, \dots, 255\}$ for the first 4 bytes. This is because, since the section string table is usually less than 256 bytes, the string table index, $V(\text{sh_name})$ should be within $\{0, 255\}$
- $V(\text{sh_type}) \in \{0, \dots, 11\}$ or it takes the other four special values such as 0x70000000 and 0x7fffffff
- $V(\text{sh_flag}) \in \{0x1, 0x2, 0x4, 0xf0000000\}$
- $V(\text{sh_addr})$ aligned with 4 bytes
- $V(\text{sh_of f set}) < L(\text{footer})$
- $V(\text{sh_size}) < L(\text{footer})$
- $V(\text{sh_link})$ and $V(\text{sh_info})$ could be 0, or I which is an index value to SHT, string table, or dynamic symbol table
- $V(\text{sh_addralign})$ is 0 or positive integral power of two
- $V(\text{sh_entsize})$ is 0 or E which is the size of the corresponding entry

From our profile, I is usually less than 13, and E is less than 11. With these value constraints, and the total number of section headers (28 in our working example), we are able to accurately locate our footer.

Searching PHT A PHT is used to locate the segments (note that a segment is composed of a few sections) that contain information necessary to create the process memory image of the program. Each program header is 32 bytes in length. In particular, for our ls binary, as depicted in Fig. 4, it has 8 program headers (specified in the ELF header) starting at 0x34. Usually, a program header starts right after the ELF headers (it will be in the same 4K block). We do not need to search to locate this. However, if necessary, we can derive the program header signatures according to its definition below, to scan for them in a manner similar to section header signature derivation.

```
typedef struct {
00 Elf32_Word p_type;
04 Elf32_Off p_offset;
08 Elf32_Addr p_vaddr;
12 Elf32_Addr p_paddr;
16 Elf32_Word p_filesz;
20 Elf32_Word p_memsz;
24 Elf32_Word p_flags;
28 Elf32_Word p_align;
} Elf32_Phdr;
```

Type	Offset	VirtAddr	PhysAddr	FileSiz	MemSiz	Flg	Align
PHDR	0x000034	0x08048034	0x08048034	0x00100	0x00100	R E	0x4
INTERP	0x000134	0x08048134	0x08048134	0x00013	0x00013	R	0x1
[Requesting program interpreter: /lib/ld-linux.so.2]							
LOAD	0x000000	0x08048000	0x08048000	0x15ea4	0x15ea4	R E	0x1000
LOAD	0x016000	0x0805e000	0x0805e000	0x00390	0x0080c	RW	0x1000
DYNAMIC	0x016014	0x0805e014	0x0805e014	0x000e8	0x000e8	RW	0x4
NOTE	0x000148	0x08048148	0x08048148	0x00020	0x00020	R	0x4
GNU_EH_FRAME	0x015dac	0x0805ddac	0x0805ddac	0x0002c	0x0002c	R	0x4
GNU_STACK	0x000000	0x00000000	0x00000000	0x00000	0x00000	RW	0x4

Fig. 4. Program headers of our ls binary.

From the program header, we first infer the base virtual address of the image file while loading into the memory. For example, as shown in Fig. 4, the first segment PHDR starts at offset 0x34 with Addr 0x8048034. We can therefore conclude that the base virtual address is $0x8048034 - 0x34 = 0x8048000$. More importantly, we can also learn each segment offset in the file, for example, INTERP segment starts at 0x134 and its content contains a string `/lib/ld-linux.so.2`. All other program code segments such as `.init`, `.plt`, and `.text` sections are at offset 0x0 with size 0x15ea4. After that, there is a data segment including sections such as `.ctors`, `.got`, `.got.plt`, `.data`, `.bss` at 0x16000, with size 0x390. We keep iterating each program header and eventually build a road map of the layout of the binary code. The output of our road map containing the place holders for every b_i except b_0 (i.e., h_i) is well-defined and filled. Our goal is to gradually fill in the content for each other b_i , where $i \in \{1, \dots, L(\text{footer})/\text{Block_Size}\}$.

3.2. Block-node linker

From the ELF header (the *header*) we can locate PHT, and using the signature we can locate the SHT (the *footer*). If there is no fragmentation, we can directly scan the disk and link b_i to its following b_{i+1} provided that we can exclude the indirect data block (using some heuristics). However, if a garbage gap exists, such an approach will fail. Thus, the most challenging part in Bin-Carver is *deciding how to link each individual b_i assuming the worst case scenario that a large volume of blocks are fragmented*.

As a result, we have to explore the internal semantic relation between b_i and b_j to “logically” connect them. For input such as text files, we may utilize word splitting heuristics to merge two blocks. However, we are facing binary code. Therefore an intuitive (but naive) approach may try to disassemble each block b_i and from the disassembled code to explore the semantics between two blocks such as the program control flow paths. However, it is very challenging to disassemble each b_i individually for x86 binary code because a legal instruction could start at arbitrary place in b_i .

Fortunately, we have a new observation: we can explore the address pair of caller–callee to fill the block place holder of caller b_{caller} and callee b_{callee} , and logically “link” b_{caller} and b_{callee} together. For example, as shown in Fig. 5, for the instruction `e8 de 00 00 00` at file offset 0x0149d (in b_1), its target address is encoded in the operand `de 00 00 00` which is $0x0149d$ (the file offset) + 5 (instruction length) + $0xde$ (operand) = $0x01580$. Then we can expect the target address at $0x01580$ to be a function prologue. Note that a function prologue usually has a signature such as `push ebp, mov esp, ebp` (for local function calls within the binary code), or a PLT table with a `jmp, push, jmp` instruction sequence (for library calls). Thus, we can search for the function prologue at an offset of 0x580 from block b_i ($i \geq 1$), and we find it is at $0x01580$ which is in PLT and still in b_1 . Then, we could “link” the two blocks together though they are both b_1 in this case.

As another example, for the last call instruction `e8 f7 f5 fe ff` at file offset 0x11e84 (virtual address 0x8059e84)

```

8049480 <_init>:
8049480: 55          push  %ebp
8049481: 89 e5      mov   %esp,%ebp
8049483: 53          push  %ebx
...
804949d: e8 de 00 00 00    call  8049580 <__gmon_start__@plt>
...
80494b0 <abort@plt-0x10>:
80494b0: ff 35 08 e1 05 08  pushl 0x805e108
80494b6: ff 25 0c e1 05 08  jmp   *0x805e10c
80494bc: 00 00          add   %al,(%eax)
...
8049580 <__gmon_start__@plt>:
8049580: ff 25 40 e1 05 08  jmp   *0x805e140
8049586: 68 60 00 00 00    push  $0x60
804958b: e9 20 ff ff ff    jmp   80494b0 <_init+0x30>
...
8059e84: e8 f7 f5 fe ff    call  8049480 <_init>
...

```

Fig. 5. Sample disassembled code from `ls`.

in Fig. 5, from the operand `f7 f5 fe ff`, we can infer the callee block from $0x11e84 + 5 + 0xffff5f7 = 0x1480$. Meanwhile, we have learned 0x1480 is in our second block b_1 , and we can directly compute the $b_{\text{caller}} = b_{11}$ because $(0x1480 - 0xffff5f7 - 5)/4096 = 11$. Then we can link b_1 to b_{11} or b_{11} to b_1 because once either node is determined, we can determine the other one. That is, the “logic” connection is bi-directional.

We could also observe that for the library call case (the first example), since we have learned the PLT block number, we can use the PLT block number as an anchor with which to identify the absolute block number of the calling block. For a local call case, we can only determine the relative distance between caller and callee block. Also, we need to emphasize that we only need to search for instruction sequences starting with `e8` (the CALL opcode) without really disassembling the binary code. There are many `e8` sequences scattered across blocks (Note that an unpacking framework Eureka (Sharif et al., 2008) also leveraged this observation for their bi-gram analysis). For example, we found 958 direct call instructions scattered across 18 blocks among the 23 blocks in total for `ls`. But we cannot use indirect calls (machine code `ff` or `9a`) because we cannot resolve the target address statically. Also, unlike a callee’s prologue-signature, we cannot use the `jmp` target because we cannot differentiate the target address since the `jmp` target could be anywhere (and there is no signature of the target as well). Additionally, in most cases we can directly use library calls to resolve all the block numbers because the number of library calls is significantly larger than local calls (for example, it is 956 vs. 22 in the `ls` binary).

3.3. Conflict-node resolver

After being processed by our *block-node linker*, a particular place holder i could have several candidate blocks. We will have to eliminate the redundant ones. Our solution is to use the already identified non-conflict nodes, which we use to explore the internal logic connections and resolve the conflict node. For example, from our b_0 (there is only one), the ELF header node, we can resolve each segment and section if there are any constraints (such as, for a string table, we would expect that the target node contains strings). If there are more than two library calls in a block, the relative distance between the PLT and the caller target

should be identical if the PLT is located in one block. Also, with more and more nodes identified, there will be more caller and callee relations, and we will keep resolving until reaching a fixed point (no node can be removed further).

Meanwhile, our *block-node linker* only focuses on linking the *code* blocks of the ELF binary. One may wonder how we handle the other *data* blocks such as data in `.data` or `.debug` sections. Actually, our *conflict-node resolver* can facilitate this. Specifically, our current Bin-Carver design is that we treat data sections as one block that is between the ELF header and the first block of the code section we identified. If the data block is fragmented, our *resolver* will explore other constraints defined in the PHT and SHT to resolve them. For instance, the `.rodata` section will be defined in the SHT, and `.rodata` is usually strings. Thus, we can first resolve the location of the `.rodata` section in the disk. This will also help identify other sections. Various `.debug` sections, if present, show the same predictable and exploitable patterns. In the worst case, if the data section does not contain any of these identifiable sections and is fragmented, then we cannot recover the data section, and we have to resort to dynamic execution to eliminate the bogus permutations. That is, we have to try the permutations of the garbage block when generating the binary files to test. If the recovered binary file does not crash during execution, then that is one sign of successful recovery. One of our future efforts will investigate other possible solutions.

3.4. Putting it all together

When given a disk image D , Bin-Carver will first remove those indirect data blocks because they are data gaps. The signature to remove them is to look for the data block in which data is well-aligned (4 bytes), for a certain chunk it contains a contiguous block number (non-decreasing), and that there is no duplicated element in the entire block (data block is not shared). It is not entirely necessary to use this signature to filter the indirect block, as our *linker* and *resolver* is able to get rid of it in most cases. However, to make our system more efficient (run faster), we use this signature approach to filter the indirect blocks.

After that, we search all the ELF headers using our ELF header *scanner*. For each ELF header h_i , we use the algorithm presented in Algorithm 1 to recover the ELF file e_i . More specifically, we first search the PLT table using the signature described in §3.2 and locate its logical block number (line 2). Next, we find the end block of our file by invoking function `SearchSectionFooter` (line 3). After that, we initialize the set for each file content block from 0 to n with an empty set (line 4 and line 5), except B_0 with the ELF-header block (line 6). Then we scan each physical block starting from ELF-header block (b_0) to the maximum block b_{Max} (line 7). If there are any library calls in the physical block (line 8), we will compute its logical block number using the PLT block number (line 9), and union the target block with this physical block (line 10). Our algorithm from line 5 to line 8 works similarly to the insertion sort algorithm (Knuth, 1997) in the sense that we both first scan the blocks and then insert the block at the right place.

Not every B_i gets filled with a block b_x , because b_x may not have library calls. Then we explore the logic gaps in two selected blocks to fill the unselected blocks. For example, if B_i

and B_k both have blocks but not B_j , then we will fill the unselected “gap” blocks to fill B_j (`HandleUnselectedNode` in line 11). After that, a particular set B_i may have multiple b , then we will explore all other constraints as described in §3.3, to eliminate the redundant nodes in B_i (`ResolveConflictNode` in line 12). Eventually, we concatenate the block content from B_i to output the final ELF file (line 13).

4. Evaluation

To demonstrate the effectiveness of this approach, we have implemented Bin-Carver using C# for our algorithm 1. A mixture of C# and Python code was used to help collect statistics and produce disk images. The entire system consists of approximately 1700 lines of code.

It is worth noting that initially we planned to compare Bin-Carver with some other state-of-the-art file carving tools such as Foremost (Foremost: a console program to recover files) and Scalpel (Richard and Roussev, 2005). However, it turns out that neither of them support carving for fragmented ELF binary files. This again demonstrates that Bin-Carver is truly a first-of-its-kind tool that offers a unique file carving capability.

4.1. Experiment setup

Sample data collection To evaluate Bin-Carver, we created 8 disk images with 2G-bytes each, and they can be classified into two sets: one (from Disk-1 to Disk-4) is the disk images without any overwritten files, the other set (from Disk-5 to Disk-8) is the disk images with multiple copy and delete rounds. In particular,

Algorithm 1 ELF-file recovery

Require: `LibCall(b)` returns a list of the library calls in a block b ; `Dist(c, plt)` returns the absolute block number of the caller block for a library call c when given PLT block number plt ; `SearchPLT(i, j)` returns the block number of the PLT table in block b_i and b_j ; `F(x)` returns the physical block content of x ; `SearchSectionFooter(b)` returns the block number of the physical disk address of the SHT searched from block b .

Input: the disk image D (which has excluded indirect data blocks), an ELF-header h_i , and the total logic block number n which is identified from either the section header offset in ELF header or the maximum file offset from the PHT.

Output: e_i , an executable file for header h_i .

```

1: ELF-Carver( $h_i, n, D$ ) {
2:    $K \leftarrow \text{SearchPLT}(0, n)$ 
3:    $Max \leftarrow \text{SearchSectionFooter}(b_0)$ 
4:   for  $j \in \{0, n\}$  do:
5:      $B_j \leftarrow \{\}$ 
6:    $B_0 \leftarrow \{b(h_i)\}$ 
7:   for  $j \in \{0, Max\}$  do:
8:     for each  $c \in \text{LibCall}(b_j)$  do:
9:        $m \leftarrow \text{Dist}(c, K)$ 
10:       $B_m \leftarrow B_m \cup \{b_j\}$ 
11:    $\text{HandleUnselectedNode}(0, Max)$ 
12:    $\text{ResolveConflictNode}(0, n)$ 
13:    $e_i \leftarrow \text{Concatenate}(B_0, B_n)$ 
14: }
```

- Disk 1 – This disk contained the contents of `/bin`. This is a small baseline sample, as it contained 117 binaries at only around 10 MB in size.
- Disk 2 – This disk contained `/bin`, `/sbin`, and `/usr/bin`. This resulting in more ELF files, for a total of 1090 binaries.
- Disk 3 – This disk contained about half the binaries from disk 2 (545 files), with another half of that unlinked before the snapshot was taken, leaving 274 binaries on disk and 271 deleted binaries remaining in the raw data.
- Disk 4 – This disk contained the entirety of disk 2 as well as some SO ELF files from `/lib`, resulting in a total of 1265 binaries.
- Disk 5 – This disk was created by first copying all of the files from disk 4 into the disk, deleting all of them, and then randomly copying half back.
- Disk 6 – This disk was created by first copying all of the files from disk 4 into the disk, deleting half of them randomly, and then copying half of the files from disk 4 back into the disk.
- Disk 7 – This disk repeated the same cycle as the previous one 2 times with smaller batches to create a messier disk image.
- Disk 8 – This disk did more unpredictable, smaller copy and delete cycles to create the most chaotic image.

Some metrics on disk image creation (such as the number of copy and remove operations) are provided along in Table 1 to help clarify the operations that went into constructing each data point. It is important to note, however, that *disk state is just as much a product of the context and order of the operations as it is the quantity*, so the descriptions of each disk's creation are important to understand as well.

More specifically, we use the following nine metrics (showing from the 2nd column to the 10th column in Table 1) to describe the characteristics of these disk images. In particular,

1. \sum **Copies** – The total executions of the `cp` command used to build the disk.
2. \sum **Removes** – The total executions of the `rm` command used to build the disk.
3. \sum **Operations** – The sum of all operations applied to the disk.

4. \sum **ELF_F** – The total number of ELF files on the disk. This is a count of the valid ELF files on the hard drive before it was unmounted and the image was created.
5. \sum **Del_F** – The total number of ELF files deleted from the disk. This is the number of ELF files which were originally on the hard drive, but were deleted at some point before the image was created.
6. \sum **Frag_F** – The total number of fragmented ELF files. This is the number of ELF files whose data block sequence contains one or more non-contiguous block pairs. In Fig. 6, this would be 3 for both collections because each one contains 3 fragmented files.
7. \sum **Breaks** – The total number of breaks in ELF data block sequences for the entire disk. This gives an idea of how many file fragments exists. For example, 2 files in 2 pieces each would result in a \sum Breaks metric of 2, but 2 files in 4 pieces each would result in a \sum Breaks metric of 6. In Fig. 6, file system *F* would have a score of 3, while file system *F'* would have a score of 6.
8. \overline{G}_F – The average garbage blocks per file among all fragmented files. This is $(1/|F|)\sum_{i \in F}|g_i|$, where *F* is the set of fragmented files and *g_i* is the set of garbage blocks in file *i*. In Fig. 6, *F* would have a score of 20.3 for this metric, while *F'* would have a score of 2.0.
9. \overline{G}_D – The average garbage blocks per file among all files in the file system. This is $(1/|D|)\sum_{i \in D}|g_i|$, where *D* is the set of fragmented files and *g_i* is the set of garbage blocks in file *i*. Since all files in Fig. 6's file systems are fragmented, this value will be the same as \overline{G}_F .

Note that all files in our system are ELF binaries. Thus, our sample data is the worst case for our recovery because all the noisy data blocks are likely to contain machine code, which significant challenges our system, especially our block-node *linker* and conflict-node *resolver* components, due to high false positive rates. We ran some tests to verify this assumption and noticed no difference in recovery accuracy between comparable disks that differed only in the addition of heterogeneous data. We tested by filling a disk to capacity with PDF, MP3, MS Office, and image files. We then deleted enough to copy the 117 ELF files that will be used by Disk 1. No change in behavior was observed.

Each testing disk image size is 2G-bytes to help cut down on variation of carving results due to disk size. The algorithm can scale up to larger disks if a few locality

Table 1
Disk statistics on the sample data.

Disk image	Disk creation			Disk characteristics					
	\sum Copies	\sum Removes	\sum Operations	\sum ELF_F	\sum Del_F	\sum Frag_F	\sum Breaks	\overline{G}_F	\overline{G}_D
Disk 1	117	0	117	117	0	38	38	1.0	0.322
Disk 2	1090	0	1090	1090	0	389	390	1.002571	0.357
Disk 3	546	273	819	545	271	190	191	1.005263	0.3498
Disk 4	1265	0	1265	1265	0	466	467	1.002164	0.3689
Average	754.5	68.25	822.75	754.25	67.75	273	271.5	1.0025	0.349425
Disk 5	1897	1265	3162	632	633	449	1449	1.004474	0.3546
Disk 6	1897	633	2530	934	317	502	1678	1.161148	0.415
Disk 7	1771	378	2149	681	584	453	800	1.5364	0.5497
Disk 8	1097	981	2078	772	319	785	955	2.065789	0.7195
Average	1665.5	814.25	2479.75	754.75	463.25	547.25	1220.5	1.44195	0.5097

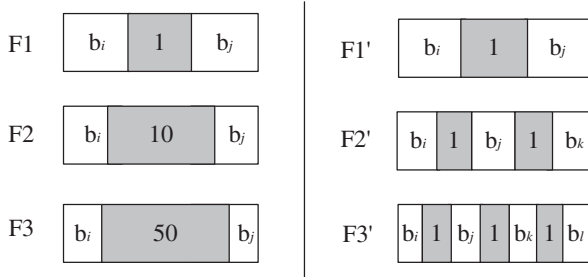


Fig. 6. Example file system fragmentation patterns: F and F' .

assumptions are made. When the distance to look for section signatures is constrained to a constant, the performance of the algorithm for each individual file is invariant with respect to the size of the disk. This means that the algorithm's performance relies only on the number of files to be recovered rather than the size of the disk.

Ground truth collection To evaluate how accurate our system is, we also need to collect the ground truth; we have to verify that our recovered files are the true ELF files. This turns out to be a challenging problem since we are performing reverse engineering. Fortunately, as when we create the disk image, we have the ground truth of the true ELF files in terms of the file contents. Thus, we can create an MD5 hash of both the first block as well as each individual block of the entire file for each true ELF binary (hashing each individual block of a file allows us to detect the true data in highly fragmented scenario), and then, for each recovered binary whose first block MD5 exists among the true ones, we can compare each individual block MD5 to ensure that the integrity was kept. This ground truth collection is in fact a file fingerprinting based recovering technique (McDaniel and Heydari, 2003).

4.2. Effectiveness

We tested Bin-Carver with the above 8 disk images for the effectiveness, in terms of the identification rate and recovery rate. More specifically, these two metrics are described in the following:

- 1. Identification Rate (IR)** – IR shows the portion we can still identify in the disk no matter how fragmented the disk is. It is defined as the proportion of *valid* files in the file system that were identified before its image was taken. For cases such as Disk 3 in which deletions occurred but no further operations were carried out, the deleted files are considered *valid*. In other cases, *deleted files are not considered valid if the hash value cannot match the original files*, as further copy operations may have overwritten part of the latent file and this will be detected by our block-based hash approach. Issues such as malformed files, extreme fragmentation, or missing Shared Object metadata can all degrade the identification ratio.
- 2. Recovery Rate (RR)** – This is the proportion of valid files in the file system before its image was taken that were identified and successfully recovered. This metric

directly shows how effective our system is with respect to the identified files.

Our effectiveness evaluation results are presented in Fig. 7. We can see that our Bin-Carver has met our expectations: it performs extremely well in extracting ELF binaries without metadata with an IR of 96.3% and RR of 93.1% on average when handling file systems ranging from pristine to chaotic highly fragmented. Additionally, on disk images 1, 2, 3, and 4, it has predictably solid low failure rates (99.85% IR, 98.1% RR). The similarity between disk 2 and 3 demonstrates that, when they remain in the disk intact, the deleted ELF files are handled without a problem.

Disk 4 only suffers a slight dip compared to disk 2, and this is due to the unreliable nature of the Shared Object files, which are not even required to have section header tables (SHT). Disks 5 through 8 show far greater fragmentation, as they were a result of attempting to contrive pathological bad cases in which not only is there heavy fragmentation, but in which the fragmentation consists of other ELF files. The disks from 5 to 8 show predictably degraded effectiveness as the disks were subjected to an increasingly lengthy battery of copy and delete operations, and disks 7 and 8 showed the greatest decline in the effectiveness due to very messy file systems. However, Bin-Carver still manages to recover a majority of the ELF files intact from the extremely chaotic images.

The failed recovery in the non-fragmented images are due to occasional files that do not match expectations. We manually examined the causes and we found these were mainly due to SO libraries that do not have section header tables, or due to the malformed ELF files. Also, there were several ELF files that, upon manual inspection, did not seem to contain data that matched their header in structure. These files obviously invalidate many of the structural assumptions made during recovery and will, as a result, not be recovered.

4.3. Performance overhead

We also tested the run-time overhead of our Bin-Carver against these disk images. The data is presented in Fig. 8. We see that the performance is split into two groups. The first three finished almost immediately, while the

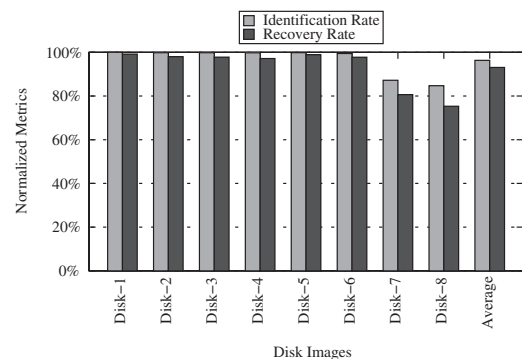


Fig. 7. Effectiveness of Bin-Carver.

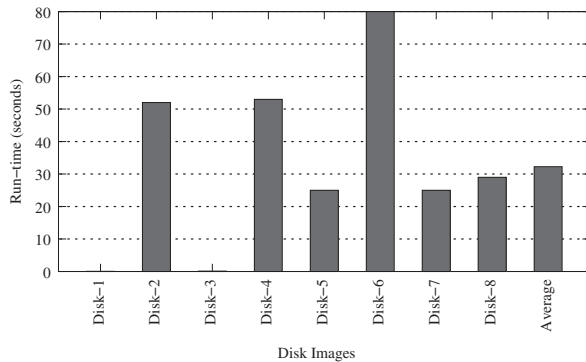


Fig. 8. Performance overhead of Bin-Carver.

remainder took half a minute to slightly over a minute to process. All performance slowdowns occur during our *linker* and *resolver* which are more computationally expensive than the rest of the recovery process. There are a few large files with wide gaps, and such gaps are detrimental to performance in these examples. This is because, when the garbage data consists of ELF binary instructions, the sheer number of caller–callee instructions that must be searched bog down the algorithm’s run time, and so any disk image containing such files will suffer performance penalties.

5. Limitation and future work

In this section we examine limitations of our Bin-Carver and propose future work to address them.

As mentioned in §1, the current focus of Bin-Carver is the recovery of ELF binaries. Though technically UNIX-ELF and Windows-PE (Microsoft pe and coff specification) share a lot of similarities in their file format design (e.g., they both have a road map description in the beginning of the file describing each program segment), there are some slight differences such as PLT (procedure linkage table in ELF) vs. IAT (import address table in PE). Our immediate future work is to address the issues relating to these differences with the goal of handling PE binary files in Bin-Carver.

While our current design assumes that an ELF-footer (i.e., the SHT) is always at the end of a file, it is possible that the ELF-footer is located in other places because ELF specification does not tell where the ELF-footer should be (Executable and linkable format). Note that we are still able to identify SHT using its signature. The only problem is just SHT might not be used as our ELF-footer any more in this case. One possible approach is to use the block right before the other file’s starting block (e.g., ELF-header) as the footer of the current to-be-recovered file. One of our future efforts will investigate how to address this problem systematically.

ELF specification also does not specify where PHT will be. To identify PHT, currently we assume it is always right after the ELF header, which is true for all the ELF binaries we tested. It is possible that PHT is located in other places. Fortunately, similarly to SHT, PHT also has clear signatures

and we are able to scan it. If we do encounter such cases, we will extend our Bin-Carver to have a PHT signature.

Finally, for large fragmented disks, our conflict-node *resolver* may not be able to remove all of the conflicted nodes. The reason is that it is possible that we will not have enough constraints to remove the garbage. For instance, if b_i and b_{i+1} has 10 garbage blocks and three of which still satisfy our constraints, then we will have four final copies. As such, another avenue of future work will design other techniques to further remove the garbage blocks. We are currently working on a dynamic validation approach which involves running and testing all the possibly recovered binaries. If the linked garbage block crashes the program, we can label it as a redundant node and eliminate it. We believe this dynamic validation approach will also help removing the garbage data blocks.

6. Related work

One of the widely used file carving programs is Foremost. It is one of the first file carvers that recovers files based on their headers, footers, and internal data structures. Scalpel (Richard and Roussev, 2005), an extended version of Foremost, is a more generalized file carving tool that aims to recover non-fragmented images. However, advancements in both Foremost and Scalpel in file carving concern performance considerations rather than resilience toward fragmentation. Additionally, they are geared toward recovering multimedia files and very little effort has been put forth toward handling binary executables, which actually directly motivated our Bin-Carver.

Garfinkel (Garfinkel, 2007) attempted to solve this fragmentation problem by examining files as potentially split into a pair indicated by the file’s header and footer. Once these endpoints are identified, different combinations of fragments pairs are exhaustively checked until the file passes some decoder’s verification algorithm. While this header-footer and verifier approach has made a large step in file carving, Anandabrata et al. (Pal et al., 2008) illustrated several problems with it. For example, this approach sometimes suffers from poor scalability: a bi-fragmented file with a large gap in between will take too long to finish. Also, validation using decoding is frequently subject to false positives or impossible to apply to a particular file type.

Another fragmentation-resilient carving approach was proposed by Pal and Memon (Pal et al., 2003) that viewed the problem graphically. They used a modified Dijkstra’s algorithm (Dijkstra, 1959) to find a shortest path between a graphical representation of the fragments. It makes a greedy choice using a weight function defined using a metric of “edge similarity” to rate transitions by the compatibility of the concatenation of the contents at the end of the start node and the beginning of the end node. An improvement was later proposed (Pal et al., 2008) for this approach, which uses a sequential hypothesis test to move through the file block by block and attempt to pinpoint the beginning and end of fragments using statistical hypothesis testing.

Recent efforts in memory forensics also explored the graph-based approach to recover data instances. In particular, exploiting the points-to relation defined in data structure definitions, SigGraph (Lin et al., 2011) shows that

we can derive a robust graph-based signatures in identifying kernel data instances. DIMSUM (Lin et al., 2012) further pushes this graph-based approach in identifying deleted data objects.

Bin-Carver shares the idea of exploring the graph connection between data blocks, but differs in the way of how to find the connections. In particular, previous work did not attempt to identify the signatures in the binary code such as our verifiable caller–callee signatures to connect the data blocks. Moreover, they did not make use of any “road map” within files and instead rely on edge compatibility.

Finally, besides the above file carving technique, as demonstrated in our experiment, we can use hash value (MD5) based technique to identify the data block in disk for known files, which was proposed by McDaniel and Heydari (McDaniel and Heydari, 2003). There are also other approaches, such as byte frequency based classification and clustering technique (Karresand and Shahmehri, 2006a, 2006b; Moody and Erbacher, 2008). Bin-Carver complements these techniques by exploring other features inside file content for the file recovery.

7. Conclusion

We have presented Bin-Carver, a tool for dissecting, mapping, and recovering binary executable files from raw binary data. The key idea is to explore the *road map information* defined in executable file headers and the *explicit control flow paths* present in the binary code, to “logically” connect the data blocks in the disk. Our experiment with thousands of binary code files has shown that our Bin-Carver is extremely accurate, and much better than all the existing file carving techniques when recovering binary files with fragmentations. In addition, Bin-Carver also provides a useful complement to the more traditional header–footer pairing approach for file carving to gain more complete disk image recovery.

Acknowledgment

We greatly appreciate our shepherd Golden G. Richard III for his tremendous help in improving the paper. We also thank the anonymous reviewers for their insightful comments and suggestions. This research was supported in part by the Air Force Office of Scientific Research (AFOSR) under Award No. FA-9550-08-1-0260. Any opinions, findings, and conclusions or recommendations in this paper are those of the authors and do not necessarily reflect the views of the AFOSR.

References

- Dijkstra EW. A note on two problems in connexion with graphs. *Numerische Mathematik* 1959;1(1):269–71.
- Dolan-Gavitt B, Srivastava A, Traynor P, Giffin J. Robust signatures for kernel data structures. In: Proceedings of the 16th ACM Conference on Computer and Communications security (CCS'09). Chicago, Illinois, USA: ACM; 2009. p. 566–77.
- Executable and linkable format, <http://wiki.osdev.org/ELF>.
- Foremost: a console program to recover files, <http://foremost.sourceforge.net>.
- Garfinkel S. Carving contiguous and fragmented files with fast object validation. In: Proceedings of the 7th Annual Digital Forensic Research Workshop (DFRWS); 2007.

- Jpeg file interchange format file format summary, <http://www.fileformat.info/format/jpeg/egff.htm>.
- Karresand M, Shahmehri N. Oscar – file type identification of binary data in disk clusters and ram pages. In: Security and Privacy in Dynamic Environments, vol. 201. IFIP International Federation for Information Processing; 2006a. p. 413–24.
- Karresand M, Shahmehri N. File type identification of data fragments by their binary structure. In: Information Assurance Workshop, 2006. IEEE; 2006b. p. 140–7.
- Knuth DE. The art of computer programming. In: Fundamental algorithms. 3rd ed., vol. 1. Redwood City, CA, USA: Addison Wesley Longman Publishing Co., Inc; 1997.
- Lin Z, Rhee J, Zhang X, Xu D, Jiang X. Siggraph: Brute force scanning of kernel data structure instances using graph-based signatures. In: Proceedings of the 18th Annual Network and Distributed System Security Symposium (NDSS'11); 2011. San Diego, CA.
- Lin Z, Rhee J, Wu C, Zhang X, Xu D. Dimsum: discovering semantic data of interest from un-mappable with confidence. In: Proceedings of the 19th Annual Network and Distributed System Security Symposium (NDSS'12); 2012. San Diego, CA.
- McDaniel M, Heydari MH. Content based file type detection algorithms. In: Proceedings of the 36th Annual Hawaii International Conference on System Sciences (HICSS'03) – Track 9, vol. 9; 2003.
- Microsoft pe and coff specification, <http://msdn.microsoft.com/en-us/windows/hardware/gg463119.aspx>.
- Moody S, Erbacher R. Sadi – statistical analysis for data type identification. In: Systematic Approaches to Digital Forensic Engineering, SADFE '08; 2008. Third International Workshop on, 2008. p. 41–54.
- Pal A, Sencar H, Memon N. Detecting file fragmentation point using sequential hypothesis testing. *Digital Invest* 2008;5(Suppl. 1).
- Pal A, Memon N. The evolution of file carving. *Signal Processing Magazine, IEEE* 2009;26(2):59–71.
- Pal A, Shanmugasundaram K, Memon N. Automated reassembly of fragmented images. In: Proceedings of the 2003 International Conference on Multimedia and Expo ICME '03, vol. 2. Washington, DC, USA: IEEE Computer Society; 2003. p. 625–8.
- Richard III GG, Roussev V. Scalpel: a frugal, high performance file carver. In: Proceedings of DFRWS 2005; 2005.
- Sharif M, Yegneswaran V, Saidi H, Porras P. Eureka: a framework for enabling static analysis on malware. In: Proceedings of the 13th European Symposium on Research in Computer Security. Malaga, Spain: LNCS; 2008.
- Year-end malware stats from av-test, <http://www.gfi.com/blog/year-end-malware-stats-from-av-test/>.

Scott Hand is a student pursuing a Master's degree in Computer Science from The University of Texas at Dallas, where he received his Bachelor's degree in Computer Science. As a recipient of the Scholarship for Service, he is preparing his security skill set for government security employment. His undergraduate research primarily focused on machine learning, and his thesis investigated probabilistic models for intelligent document retrieval. His current research interests include machine learning, digital forensics, software exploitation, and reverse engineering.

Zhiqiang Lin is an assistant professor in the Computer Science Department of The University of Texas at Dallas. He received his Ph.D. from Purdue University in 2011. His current research focuses on system and software security with an emphasis on binary code reverse engineering, vulnerability discovery, malicious code analysis, and OS kernel protection.

Guofei Gu is an assistant professor in the Department of Computer Science & Engineering at Texas A&M University. He received his Ph.D. from Georgia Tech in 2008. His research interests are in network and system security, such as botnet analysis/detection/defense, web and social network security, security in software-defined networks, and intrusion detection. Dr. Gu is a recipient of NSF CAREER award and a co-recipient of IEEE Symposium on Security & Privacy (Oakland'10) best student paper award.

Bhavani Thuraisingham (aka Dr. Bhavani) is the Louis A. Beecherl, Jr. I Distinguished Professor in the Erik Jonsson School of Engineering and Computer Science at The University of Texas at Dallas. She is an elected Fellow of the IEEE, the AAAS, and the BCS (British Computer Society). She is the recipient of numerous awards including the IEEE Computer Society's 1997 Technical Achievement Award and the 2010 ACM SIGSAC Outstanding Contributions Award. Her current research interests include data security and privacy and data mining for counter-terrorism.